COMMUNICATION

Supported Rh-phosphine complex catalysts for continuous gas-phase decarbonylation of aldehydes†

Phillip Malcho,[a] Eduardo J. Garcia-Suarez,[a] Uffe Vie Mentzel,[a] Christian Engelbrekt[b] and Anders Riisager*[a]

Heterogeneous silica supported rhodium-phosphine complex catalysts are employed for the first time in the catalytic decarbonylation of aldehydes in continuous gas-phase. The reaction protocol is exemplified for the decarbonylation of *p*-tolualdehyde to toluene and further extended to other aromatic and aliphatic aldehydes achieving excellent results in terms of both conversion and selectivity.

1. Introduction

Selective catalytic removal of carbonyl groups from molecules by decarbonylation is an important transformation in synthetic chemistry and biology.[1] In organic synthesis, for example, an aldehyde can be utilized as an *in situ* CO source for a desired carbonylation reaction, *e.g.* in a tandem approach, thus avoiding hazardous CO gas as an external reagent.[2] Selective decarbonylation constitutes also a potential strategy for the mild upgrading of carbohydrates and furanic compounds contained in biomass to bio-fuels and higher-value chemical building blocks. Such a strategy can be envisaged to be a viable alternative in bio-refineries to current deoxygenation methodologies relying on dehydration or hydrogenolysis.[3]

The selective catalytic decarbonylation of aromatic and aliphatic aldehydes with rhodium complex catalysts was introduced in the mid 1960s by Tsuji and Ohno using stoichiometric amounts of the Wilkinson catalyst, Rh(PPh₃)₃Cl, at room temperature.[4] Later, Doughty and Pignolet developed a procedure for the decarbonylation of aldehydes using catalytic amounts of the Wilkinson catalyst at high temperatures, typically 115–180 °C.[5] Only in the 1990s was it discov-

ered that complexes of rhodium and polydentate ligands provided improved yields of decarbonylation products from aldehydes when reacted in boiling dioxane.[6,7] Subsequently, Madsen *et al.* performed a thorough investigation on such rhodium catalyzed reactions monitoring the effect of mono- and multidentate phosphine ligands.[7a] In this work, they concluded that bidentate phosphine ligands in combination with Rh gave the most efficient catalyst for the studied reaction; however, high temperature of approx. 160 °C was a prerequisite.[7d] Recently, exploratory decarbonylation studies have further been performed using other transition metals *e.g.* iron, platinum or palladium in combination with phosphine ligands as catalysts with good results.[9] Despite the efforts it is yet not unraveled if these – or the established rhodium catalyzed reactions – can be carried out in continuous flow systems using heterogenized catalyst formulations. Such systems can be expected to be highly desirable on an industrial scale compared to homogeneous reaction systems, due to the ease of separation of products and versatile catalyst use.

In this study, we have examined silica-supported rhodium-phosphine and iridium-phosphine complex catalysts for continuous flow, gas-phase decarbonylation of aromatic and aliphatic aldehydes. Excellent results in terms of both activity and selectivity were obtained. The best catalytic system [Rh(dppp)₂]Cl (dppp: 1,2-bis(diphenylphosphino)propane) was found to be stable for at least 4 h with different substrates under the examined continuous flow conditions.

2. Experimental

2.1 Materials

All chemicals were purchased from Sigma-Aldrich and used without purification unless otherwise noted. The metal compounds used for catalyst preparation were prepared under an inert atmosphere of Argon (grade 5.0, Air Liquide) as described in the literature.[8,10] Silica-90 support (BET = 340 m² g⁻¹; pore volume = 0.95 cm³ g⁻¹; pore size = 90 Å; particle size = 70–230 MESH) was calcined for 4 h at 600 °C, dried under vacuum at 110 °C for 24 h and kept under moisture free conditions prior

[a]*Centre for Catalysis and Sustainable Chemistry, Department of Chemistry, Technical University of Denmark, DK-2800 Kgs, Lyngby, Denmark.*
E-mail: ar@kemi.dtu.dk; Fax: +45 45883136; Tel: +45 45252233
[b]*Department of Chemistry, Technical University of Denmark, DK-2800 Kgs, Lyngby, Denmark*
†Electronic supplementary information (ESI) available. See DOI: 10.1039/c4dt01629g

to its use. The concentrations of CO and CO_2 in the effluent were determined by a BINOS instrument placed after condensation of liquids in a cold trap kept at 0 °C.

2.2 Catalyst preparation

The supported silica catalysts $[Rh(dppp)_2]Cl/SiO_2$, $RhCl_3 \cdot xH_2O/SiO_2$, $[Rh(COD)Cl]_2/SiO_2$ and $[Ir(dppp)_2]Cl/SiO_2$ were prepared by impregnation using the following procedure: a 10 ml Schlenk flask was charged with 1.5 ml of dichloromethane and 1.5 ml of ethanol followed by the appropriate amount of a metal compound to obtain the desired metal content. The solution was then stirred for 15 min to ensure complete solvation, where after 1.0 g of silica support was added and the suspension stirred for 1 h. Finally, the volatile solvents were removed under vacuum at 70 °C over a period of 30 min to obtain the supported catalyst. The catalyst was kept under an inert atmosphere of Argon until its use.

2.3 Catalyst characterization

Thermal stabilities of the catalysts were determined by thermogravimetric analysis (TGA) on a combined TGA/DSC, Mettler Toledo, STAR^E System with a GC100 gas controller. The heating rate was 5 °C min^{-1} from room temperature to 260 °C, where the temperature was kept for 6 h.

Attenuated total reflectance infrared (ATR-IR) spectra of the catalysts were recorded on a Thermo Scientific, Nicolet iS5 spectrophotometer with a Specac Golden Gate ATR diamond cell. The spectra were recorded in the range of 4000–400 cm^{-1} with a resolution of 2 cm^{-1}.

The BET surface areas of the support and the catalysts were derived from the nitrogen adsorption–desorption isotherms performed at −196 °C (liquid nitrogen) in a Micromeritics ASAP 2020 pore analyzer. Prior to measurement, samples were degassed overnight by heating at 200 °C *in vacuo* (<10^{-4} Pa) to ensure a clean surface before adsorption.

The structure and morphology of the catalysts were examined by transmission electron microscopy (TEM) on a Tecnai G2 T20 from FEI Company (Oregon, USA) before and after decarbonylation. Prior to analysis the samples were crushed into a fine powder and subsequently supported on plain carbon film coated copper grids purchased from Agar Scientific (Stansted, UK). Elemental analysis was achieved by energy dispersive X-ray spectroscopy (EDX) using an X-Max^N detector from Oxford Instruments (Abingdon, UK).

2.4 Catalytic reactions under continuous gas-phase flow

In a typical experiment, 300 mg of catalyst was placed between two quartz wool plugs in a stainless steel, fixed-bed reactor having an inner diameter of 7 mm. The selected substrate was introduced into the reactor by a HPLC pump diluted to 50 vol% in 2-propanol or *n*-pentane at a flow rate of 0.05 ml min^{-1} *via* heated lines and evaporated before reaching the reactor. The reactor was heated by an electric furnace to the desired reaction temperature measured through a thermocouple positioned inside the oven close to the catalyst bed. Helium (grade 5.0, Air Liquide Denmark) was used as a carrier gas with a flow

rate of 10 ml min^{-1}, and the reaction pressure was 1 bar in all experiments. The product mixture was condensed directly below the reactor in a condenser kept at 0 °C and analyzed offline by GC-FID using a HP 5890 Series II chromatograph equipped with a SGE BP1 non-polar 100% dimethyl polysiloxane capillary column (50 m × 0.32 mm × 0.25 ml). Standard curves were used to quantify the conversion and product yield.

2.5 Metal depletion analysis

The condensed reaction mixtures were subjected to Inductively Coupled Plasma (ICP) analysis using a Perkin-Elmer Elan 6000 ICP-MS equipped with a cross-flow nebulizer with a LOD of 1 ng kg^{-1} to evaluate for rhodium metal leaching from the catalysts during reaction. Quantification of rhodium was made using a series of rhodium standards.

3. Results and discussion

The prepared supported catalysts with rhodium/iridium complexes immobilized on silica were tested for the very first time in continuous flow gas-phase decarbonylation of aromatic and aliphatic aldehydes. When the catalysts were tested at 250 °C in runs lasting up to 4 hours the yield was found to depend on the metal, the ligand employed and/or the metal loading. The results are compiled in Table 1.

Since $[Rh(dppp)_2]Cl$ is known to efficiently decarbonylate aldehydes under homogeneous conditions,[7] it was selected as the optimal candidate for testing it in continuous flow after being supported on silica by a simple impregnation method. Firstly, the influence of metal loading from 0.3 to 3 wt% was studied. As expected, the toluene yield increased with metal loading from 18 to 74% after 1 h of reaction confirming the rhodium metal to be catalytically active under continuous flow reaction conditions (Table 1, entries 1 and 3). Due to the high reaction temperature and in order to avoid possible issues related with the decomposition of the employed catalysts, the catalytic reaction was performed at a lower temperature (215 °C) (Table 1, entry 2) showing low to non-activity, hence it was decided to perform the decarbonylation reaction at 250 °C. Then, other Rh precursors were employed containing Cl^- and COD (1,5-cyclooctadiene) as ligands in order to study the influence of the presence of a phosphine ligand in the catalytic system (Table 1, entries 4 and 5). $RhCl_3 \cdot xH_2O/SiO_2$ gave toluene yield of 17% (TOF = 234 h^{-1}) after 1 h reaction which was comparable to $[Rh(dppp)_2]Cl/SiO_2$ (Table 1, entries 1 and 4), whereas $[Rh(COD)Cl]_2/SiO_2$ gave by far the lowest yield of only 3% (TOF = 42 h^{-1}). It is noteworthy that the $RhCl_3 \cdot xH_2O/SiO_2$ catalyst was deactivated after 1 h of reaction, while the $[Rh(dppp)_2]Cl/SiO_2$ catalyst with the dppp ligand maintained its activity for at least 4 h (Table 1, entries 1 and 4). This point signifies the important role of the ligand in catalyst stabilization during the course of the reaction.

After confirming that the best catalytic activity was obtained with the $[Rh(dppp)_2]Cl/SiO_2$ (TOF = 246 h^{-1}) catalyst, the corresponding iridium catalyst was also tested in the

Table 1 Decarbonylation of aldehydes with supported silica catalysts[a]

| Entry	Catalyst	Metal (wt%)	Substrate	Yield[b,c] (%)	Yield[d] (%)	TOF[b] (h^{-1})
1	[Rh(dppp)$_2$]Cl/SiO$_2$	0.3	p-Tolualdehyde	18	25	246
2[e]	[Rh(dppp)$_2$]Cl/SiO$_2$	0.3	p-Tolualdehyde	3	5	42
3	[Rh(dppp)$_2$]Cl/SiO$_2$	3	p-Tolualdehyde	74	53	102
4	RhCl$_3$·xH$_2$O/SiO$_2$	0.3	p-Tolualdehyde	17	5	234
5	[Rh(COD)Cl]$_2$/SiO$_2$	0.3	p-Tolualdehyde	3	1	42
6	[Ir(dppp)$_2$]Cl/SiO$_2$	3	p-Tolualdehyde	23	2	30
7	[Rh(dppp)$_2$]Cl/SiO$_2$	3	o-Tolualdehyde	95	83	132
8	[Rh(dppp)$_2$]Cl/SiO$_2$	3	m-Tolualdehyde	31	9	42
9	[Rh(dppp)$_2$]Cl/SiO$_2$	3	p-Anisaldehyde	56	44	80
10	[Rh(dppp)$_2$]Cl/SiO$_2$	3	1-Nonanal	94	85	126
11[f]	[Rh(dppp)$_2$]Cl/SiO$_2$	3	p-Tolualdehyde	80	57	114
12	SiO$_2$	0	p-Tolualdehyde	0	0	0

[a] Reaction conditions: 300 mg catalyst, 0.05 ml min^{-1} liquid flow (50 vol% of substrate in 2-propanol), 10 ml min^{-1} He as carrier gas, $p = 1$ bar, $T = 250$ °C. [b] After 1 h. [c] Selectivity towards the decarbonylation product >99% for all tested substrates. [d] After 4 h. [e] 215 °C. [f] n-Pentane was employed as the solvent.

continuous flow set-up, as such catalysts also previously have proven active for decarbonylation (Table 1, entry 6).[9b] Compared to the 3 wt% Rh catalyst (Table 1, entry 3) [Ir(dppp)$_2$]Cl/SiO$_2$ showed much lower catalytic activity yielding only 23% toluene (TOF = 30 h^{-1}) after 1 h reaction. This result can be rationalized by inspection of FTIR spectra of the two catalysts measured before and after reaction, respectively, where a characteristic peak at $\nu = 700$ cm^{-1} belonging to the ligand (dppp) disappeared after the reaction (see ESI, S1†). In addition, the spectra showed that the phosphine was removed to a larger extent from the iridium center than the rhodium center as the signal from the Ir sample collided with the signal for the pure silica.

The results obtained with the [Rh(dppp)$_2$]Cl/SiO$_2$ catalyst with p-tolualdehyde (Fig. 1, (**3**)) encouraged us to test the versatility of the prepared catalyst with other aromatic and aliphatic aldehydes. Thus, the analogous o- and m-tolualdehyde (**1**) and (**2**) were also used to study steric effects on the catalytic activity. In addition, related aromatic aldehydes with both electron donor (**4**) and electron withdrawing groups (**5**)–(**9**) in the

para-position were attempted and tested under the reaction conditions. Unfortunately, the aromatic aldehydes with electron withdrawing groups (**5**)–(**9**) were poorly soluble in the applied solvents (i.e. 2-propanol and n-pentane) to provide comparable data. The obtained results are summarized in Table 1 (entries 7 to 10).

When the more electronically activated substrates with ortho and para substituents were applied, larger conversion was obtained compared to the meta-substituted tolualdehydes. Previously it has been shown for homogeneous decarbonylation reactions with Rh-complexes that upon addition of electron withdrawing substituents to the aromatic ring reaction rates are increased.[7d] This is further elaborated when the methyl substituent was exchanged with a methoxy group. However, in the current study with an immobilized catalyst the activity was apparently 25% lower for p-anisaldehyde than for p-tolualdehyde resulting in TOFs of 80 and 102 h^{-1}, respectively. On the other hand, the higher activity towards o-tolualdehyde decarbonylation (Table 1, entry 7; TOF = 132 h^{-1}) was possibly related to steric hindrance induced by the methyl
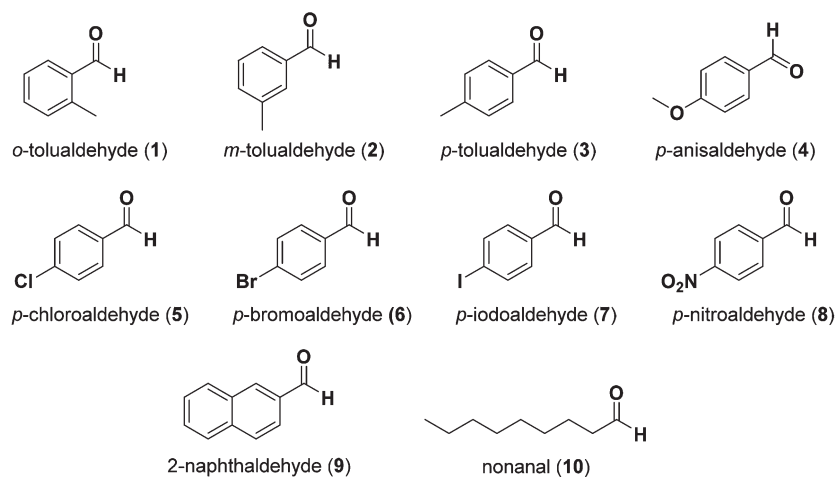
Fig. 1 Aldehydes applied for the decarbonylation reaction.

group in the *ortho*-position, thus making the expected rate-determining reductive elimination step more facile yielding the desired product.

In order to extend the scope of the continuous flow decarbonylation process and the versatility of our catalysts, an aliphatic aldehyde, namely *n*-nonanal (Fig. 1 (**10**)) was also tested under the selected reaction conditions. Excellent results were obtained with a TOF as high as 126 h^{-1} (Table 1, entry 10). A blank experiment was also carried out in the absence of the Rh complex and as expected no conversion was observed after the reaction time (Table 1, entry 12).

To get additional information on catalyst stability the continuous decarbonylation were performed with the aldehyde substrates for 4 h. Fig. 2 shows the product yields obtained as a function of time-on-stream. The best results (and catalyst stability) were attained in the decarbonylation of *o*-tolualdehyde and *n*-nonanal resulting in approx. 95% yield during the

first 2 h of reaction, before the activity decreased to around 85% after an additional hour of reaction in both the cases. A similar trend in activity decrease was also noticed for the other tested substrates.

In order to determine if the loss in activity over the 4 h reaction period was related to metal depletion from the catalysts, representative reaction samples from *n*-nonanal decarbonylation were collected after each reaction hour and analyzed by ICP-MS. The results revealed Rh amounts of 7, 11, 5 and 3 ppb, respectively, corresponding to a negligible total metal depletion of 0.04% of the initial Rh content. Thus, metal depletion did not cause the observed activity decay. In order to examine the deactivation behavior more closely, the best performing catalyst, [Rh(dppp)$_2$]Cl/SiO$_2$, was further subjected to TEM (Fig. 3) and EDX analysis (ESI, S2 and S3†) before and after catalytic reaction. As can be seen by TEM, the porous structure of the silica support was evident in the catalyst before decarbonylation (Fig. 3a). EDX of the catalyst (based on six separate measurements) revealed a homogeneous element distribution of Rh and P on the support and a Rh content of 2.0 ± 0.3 mol% before the reaction. This Rh loading was preserved (2.2 ± 0.3 mol%) after reaction, while the P/Rh molar ratio was found to be lowered from 3.4 ± 0.3 before the reaction to 2.7 ± 0.4 after the reaction (*i.e.* about 20% mass loss). The decrease in P/Rh molar ratio correlated with the activity loss observed during catalysis as a function of time, and can thus most likely be connected to ligand degradation under the applied reaction conditions (250 °C). The thermal instability of the ligand was confirmed by supplementary TGA measurements performed with the [Rh(dppp)$_2$]Cl/SiO$_2$ catalyst (ESI, S4†). Here a mass loss corresponding to approximately 10 wt% was found during heating up to 260 °C, which correlated very well with about 20% of the phosphine ligand being lost.

As is evident from the TEM pictures, the Rh-ligand complex decomposition during catalysis resulted in the generation of Rh nanoparticles with an average size of 3.2 ± 0.7 nm (Fig. 3b). The generated nanoparticles had high crystallinity with a face-centered cubic (FCC) structure (ESI, S5†). The corresponding

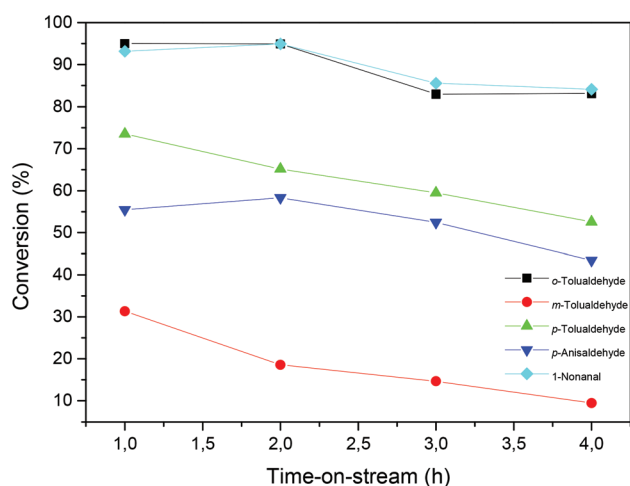**Fig. 2** Yield of products as a function of time after decarbonylation reactions with [Rh(dppp)$_2$]Cl/SiO$_2$ (3 wt% Rh). Reaction conditions: 300 mg catalyst, 0.05 ml min^{-1} liquid flow (50 vol% of substrate in 2-propanol), 10 ml min^{-1} He as carrier gas, p = 1 bar, T = 250 °C.

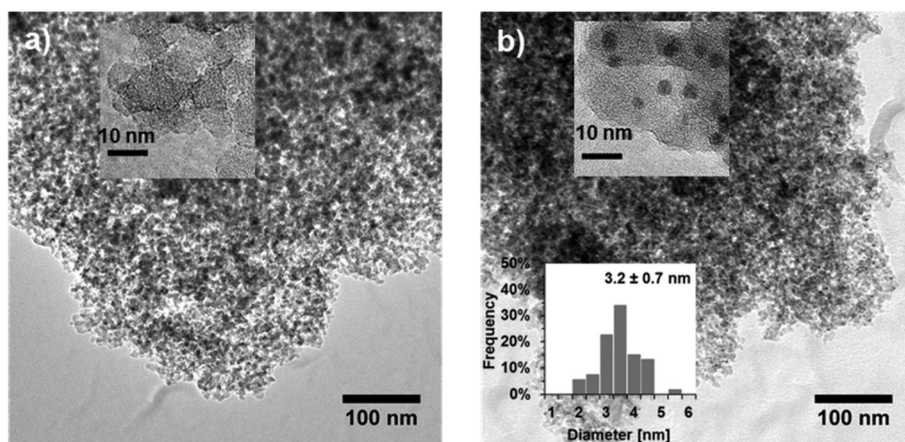**Fig. 3** TEM micrographs of the [Rh(dppp)$_2$]Cl/SiO$_2$ (3 wt% Rh) catalyst (a) before and (b) after decarbonylation. A histogram of determined Rh nanoparticle sizes is inserted in (b).
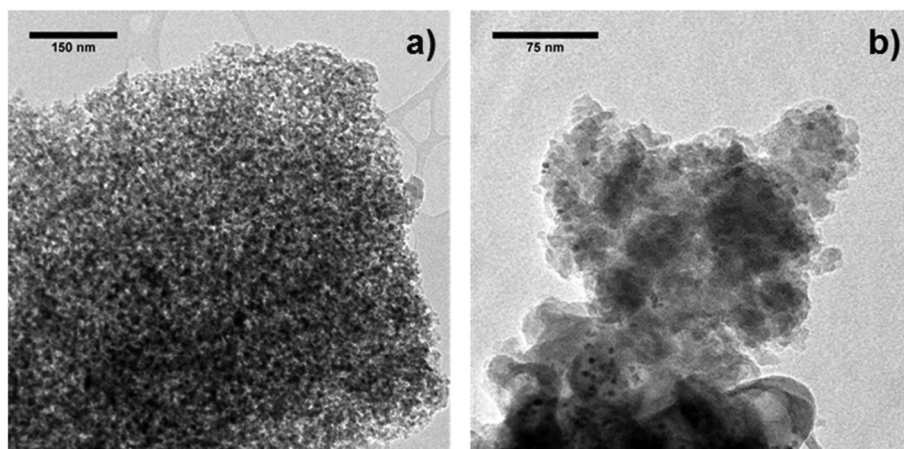
Fig. 4 TEM micrographs of the [Rh(dppp)₂]Cl/SiO₂ (3 wt% Rh) catalyst (a) before and (b) after decarbonylation reaction in *n*-pentane.

Fast Fourier Transformations (FFT) revealed inter planar distances of 1.96 and 2.80 Å, respectively, which are in good agreement with the values of the (200) and (110) atomic planes for metallic Rh.[10] To examine if Rh nanoparticle formation was facilitated by 2-propanol – which is a well-known hydrogen donor – prior to the decarbonylation reaction, and to rule out a possible contribution to the observed catalytic activity, an analogous decarbonylation experiment was performed using *n*-pentane as a solvent where formation of Rh nanoparticles is unlikely before the decarbonylation reaction. The results employing *n*-pentane were similar to the ones obtained using 2-propanol as the solvent (Table 1, entries 3 and 11), suggesting that the formation of Rh nanoparticles occurred during the course of the decarbonylation reaction, leading to decay in the catalytic activity with time and not prior to the decarbonylation reaction. In Fig. 4, TEM images of the catalyst before and after reaction are shown. It is clear that metal nanoparticles are formed during the course of the reaction as shown in Fig. 4b. Hence, the observed catalyst instability can be linked to catalyst decomposition leading to the generation of metal nanoparticles and dppp ligand loss during the course of the reaction, which in turn affects the catalytic performance negatively.

4. Conclusions

This work reports the first selective decarbonylation gas-phase reaction conducted in a continuous flow setup using silica-supported rhodium- and iridium-phosphine catalysts. Several aromatic and aliphatic aldehydes were applied successfully in the decarbonylation process. The catalytic performance was found to be influenced by both electronic and steric effects of the substrates. The preservation of the intact metal-ligand centers was found to play a pivotal role for the catalytic performance, since ligand dissociation leads to catalyst deactivation and formation of less active metal nanoparticles. The current work is being carried out in order to increase the stability of the catalytic system as well as to implement the process for other high demanded substrates.

Acknowledgements

References

1 (*a*) T. M. Cheesbrough and P. E. Kolattukudy, *Proc. Natl. Acad. Sci. U. S. A.*, 1984, **81**, 6613; (*b*) M. Dennis and P. E. Kolattukudy, *Proc. Natl. Acad. Sci. U. S. A.*, 1992, **89**, 5306; (*c*) A. Schirmer, M. A. Rude, X. Li, E. Popova and S. B. del Cardayre, *Science*, 2010, **329**, 559; (*d*) D. Das, B. E. Eser, J. Han, A. Sciore and E. N. G. Marsh, *Angew. Chem., Int. Ed.*, 2011, **50**, 7148.

2 (*a*) C. M. Jensen, K. B. Lindsay, R. H. Taaning, J. Karaffa, A. M. Hansen and T. Skrydstrup, *J. Am. Chem. Soc.*, 2005, **127**, 6544; (*b*) G. K. Min, D. Hernandez, A. T. Lindhardt and T. Skrydstrup, *Org. Lett.*, 2010, **12**, 4716; (*c*) P. Hermange, A. T. Lindhardt, R. H. Taaning, K. Bjerglund, D. Lupp and T. Skrydstrup, *J. Am. Chem. Soc.*, 2011, **133**, 6061; (*d*) S. T. Friis, R. H. Taaning, A. T. Lindhart and T. Skrydstrup, *J. Am. Chem. Soc.*, 2011, **133**, 18114; (*e*) K. Bjerglund, A. T. Lindhardt and T. Skrydstrup, *J. Org. Chem.*, 2012, **77**, 3793; (*f*) D. U. Nielsen, K. Neumann, R. H. Taaning, A. T. Lindhardt, A. Modvig and T. Skydstrup, *J. Org. Chem.*, 2012, **77**, 6155; (*g*) A. T. Lindhardt, R. Simonssen, R. H. Taaning, T. M. Gogsig, G. N. Nilsson, G. Stenhagen, C. S. Elmore and T. Skrydstrup, *J. Labelled Compd. Radiopharm.*, 2012, **55**, 411; (*h*) T. Ueda, H. Konishi and K. Manabe, *Angew. Chem., Int. Ed.*, 2013, **52**, 8611; (*i*) T. Ueda, H. Konishi and

K. Manabe, *Org. Lett.*, 2012, **14**, 3100; (*j*) T. Fujihara, T. Hosoki, Y. Katafuchi, T. Iwai, J. Terao and Y. Tsuji, *Chem. Commun.*, 2012, **48**, 8012.

3 (*a*) J. J. Bozell and G. R. Petersen, *Green Chem.*, 2010, **12**, 539; (*b*) P. Gallezot, *Chem. Soc. Rev.*, 2012, **41**, 1538; (*c*) P. N. R. Vennestrøm, C. M. Osmundsen, C. H. Christense and E. Taarning, *Angew. Chem., Int. Ed.*, 2011, **50**, 10502.

4 (*a*) J. Tsuji and K. Ohno, *Tetrahedron Lett.*, 1965, **6**, 3969; (*b*) K. Ohno and J. Tsuji, *J. Am. Chem. Soc.*, 1968, **90**, 99.

5 D. H. Doughty and L. H. Pignolet, *J. Am. Chem. Soc.*, 1978, **100**, 7083.

6 C. M. Beck, S. E. Rathmill, Y. J. Park, J. Chen and R. H. Crabtree, *Organometallics*, 1999, **18**, 5311.

7 (*a*) R. N. Monrad and R. Madsen, *J. Org. Chem.*, 2007, **72**, 9782; (*b*) E. Taarning and R. Madsen, *Chem. – Eur. J.*, 2008, **14**, 5638; (*c*) M. Kreis, A. Palmelund, L. Bunch and R. Madsen, *Adv. Synth. Catal.*, 2006, **348**, 2148; (*d*) P. Fristrup, M. Kreis, A. Palmelund, P.-O. Norrby and R. Madsen, *J. Am. Chem. Soc.*, 2008, **130**, 5206.

8 B. R. James and D. Mahajan, *Can. J. Chem.*, 1979, **57**, 180.

9 (*a*) F. M. A. Geilen, T. Vom Stein, B. Engendahl, S. Winterle, M. A. Liauw, J. Klankermayer and W. Leitner, *Angew. Chem., Int. Ed.*, 2011, **50**, 6831; (*b*) T. Iwai, T. Fujihara and Y. Tsuji, *Chem. Commun.*, 2008, 6215; (*c*) S. Maetani, T. Fukuyama, N. Suzuki, D. Ishihara and I. Ryu, *Chem. Commun.*, 2012, **48**, 2552; (*d*) A. Modak, A. Deb, T. Patra, S. Rana, S. Maity and D. Maiti, *Chem. Commun.*, 2012, **48**, 4253.

10 J. W. Arblaster, *Platinum Met. Rev.*, 1997, **41**, 184.